

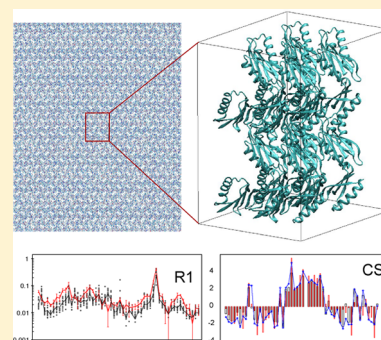
## Atomic-Resolution Structural Dynamics in Crystalline Proteins from NMR and Molecular Simulation

Luca Mollica,<sup>†</sup> Maria Baias,<sup>‡</sup> Józef R. Lewandowski,<sup>§</sup> Benjamin J. Wylie,<sup>⊥</sup> Lindsay J. Sperling,<sup>#</sup> Chad M. Rienstra,<sup>||</sup> Lyndon Emsley,<sup>‡</sup> and Martin Blackledge<sup>\*,†</sup><sup>†</sup>Protein Dynamics and Flexibility, Institut de Biologie Structurale, CEA, CNRS, UJF-Grenoble 1, 41 Rue Jules Horowitz, Grenoble 38027, France<sup>‡</sup>CNRS/ENS-Lyon/UCB-Lyon 1, Centre de RMN à Très Hauts Champs, Université de Lyon, 5 rue de la Doua, 69100 Villeurbanne, France<sup>§</sup>Department of Chemistry, University of Warwick, Gibbet Hill Road, Coventry CV4 7AL, United Kingdom<sup>⊥</sup>Department of Chemistry, Columbia University, 3000 Broadway, New York, New York 10027, United States<sup>#</sup>Lawrence Berkeley National Laboratory, 1 Cyclotron Road, Berkeley, California 94720, United States<sup>||</sup>Department of Chemistry, University of Illinois at Urbana–Champaign, 600 South Mathews Avenue, Urbana, Illinois 61801, United States

## S Supporting Information

**ABSTRACT:** Solid-state NMR can provide atomic-resolution information about protein motions occurring on a vast range of time scales under similar conditions to those of X-ray diffraction studies and therefore offers a highly complementary approach to characterizing the dynamic fluctuations occurring in the crystal. We compare experimentally determined dynamic parameters, spin relaxation, chemical shifts, and dipolar couplings, to values calculated from a 200 ns MD simulation of protein GB1 in its crystalline form, providing insight into the nature of structural dynamics occurring within the crystalline lattice. This simulation allows us to test the accuracy of commonly applied procedures for the interpretation of experimental solid-state relaxation data in terms of dynamic modes and time scales. We discover that the potential complexity of relaxation-active motion can lead to significant under- or overestimation of dynamic amplitudes if different components are not taken into consideration.

**SECTION:** Biophysical Chemistry and Biomolecules



Protein motions occurring on the pico- to millisecond time scale modulate interactions between physiological partners and are therefore of fundamental biological importance.<sup>1</sup> Nuclear magnetic resonance (NMR) relaxation measurements in solution provide detailed information about motions on time scales faster than the rotational diffusion time,<sup>2,3</sup> and motions in the nano- to millisecond range can be obtained from residual dipolar couplings.<sup>4,5</sup> Site-specific relaxation rates measured in proteins in the solid state can in principle detect molecular motions occurring on time scales up to and beyond the microsecond, stimulating considerable activity to develop appropriate strategies to achieve this end.<sup>6–20</sup>

Advances in molecular simulation of protein dynamics have regularly informed our understanding of experimental NMR data in solution.<sup>21,22</sup> However, with the notable exception of a 50 ns trajectory of the unit cell of SH3,<sup>11</sup> molecular dynamics (MD) simulations that specifically account for the crystal lattice have rarely been combined with experimental data from crystalline proteins. In this study, we compare experimentally determined dynamic parameters to values calculated from a 200 ns MD simulation of protein GB1<sup>23</sup> in its crystalline form, providing new insight into the behavior of commonly

applied approaches to the dynamic analysis of solid-state protein NMR data.

In order to correctly represent the intermolecular contacts and the periodicity present in the crystals, a “superlattice” of 32 distinct proteins (equivalent to 8 unit cells of 4 proteins each) was arranged according to the crystallographic symmetry in a periodic simulation box<sup>24</sup> (Figure 1), and a 200 ns MD simulation was performed (Supporting Information). The stability of the simulation was measured via the coordinate rmsd (Figure 1) for all 32 copies, indicating that the starting conformation was stable throughout the simulation. Unit cell dimensions are effectively constant over the entire simulation (Supporting Information), while backbone rms fluctuations (Figure 1) resemble the distribution of B-factors determined from X-ray diffraction.<sup>23</sup>

Chemical shifts are also sensitive reporters of local structural fluctuations on time scales up to the millisecond

**Received:** October 10, 2012

**Accepted:** November 23, 2012

**Published:** November 23, 2012

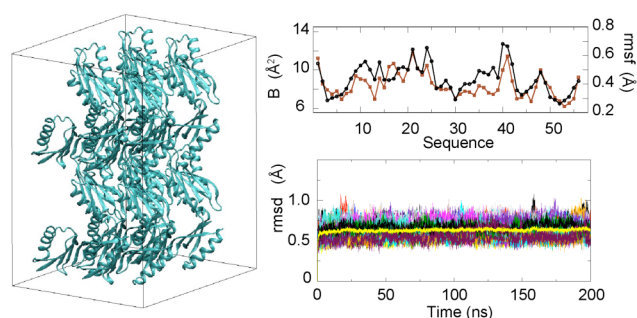


**Figure 1.** Crystalline lattice of GB1 used in the MD simulation. Thirty-two copies of the protein were simulated. Right (top): Comparison of experimental  $^{13}\text{C}$  B-factors from X-ray structure 2GI9 (black) and  $^{13}\text{C}$  rms fluctuations (red). Right (bottom): Backbone rmsd of the 32 copies compared to the X-ray conformation 2GI9. The average rmsd is shown in yellow.

and have been successfully used in comparison to MD simulation to study conformational dynamics in the solution state.<sup>25–28</sup> In order to further probe the relevance of the motions observed in the simulation, we have extracted snapshots from throughout the trajectory and for each copy of the protein and calculated expected  $^{13}\text{C}$ ,  $^{15}\text{N}$ , and  $^1\text{H}$  backbone chemical shifts using the program SHIFTX.<sup>29</sup> Average secondary shifts are compared to experimental values in Figure 2. Dynamic averaging over all substates systematically improves data reproduction compared to the individual snapshots. We also find an overall improvement of averaged shifts compared to the X-ray crystallographic structure. Inclusion of nearest-neighboring proteins in the calculation

of chemical shifts from the central copy of the protein also improves prediction of chemical shifts compared to the isolated protein, in particular, for  $\text{C}'$  shifts, probably because these nuclei are involved in the intermonomer hydrogen bonds mediating the main crystal contact. Similar results were derived when using alternative prediction algorithms.<sup>30</sup> Agreement between experiment and prediction is of similar quality to that found for soluble proteins using simulations of comparable length,<sup>25–28</sup> again providing support for the overall levels of disorder sampled in the trajectory.

Protein dynamics can also be studied by measuring NMR spin relaxation. Data are commonly interpreted using model-free mathematical models of the autocorrelation functions  $C(t)$  describing the angular fluctuations of the relaxation-active interactions. These approaches derive, by direct analogy, from expressions commonly used in solution-state NMR. The behavior and relevance of these expressions have not been tested for proteins in the solid state using MD simulation. Here, we compare relaxation rates calculated from MD to experimental values and use the trajectories of GB1 to investigate the ability of the model-free approach to capture the dynamic features present in the simulation.

Angular autocorrelation functions were calculated to compare the motional properties of  $\text{N}-^1\text{H}$  bond vectors in the simulation to experimentally determined parameters. Relaxation rates can be conveniently predicted directly from simulation by expressing the  $C(t)$  as a sum of weighted exponential terms.<sup>31,32</sup>

$$C(t) = A_0 + \sum_{k=1}^n A_k e^{-t/\tau_k} \quad (1)$$

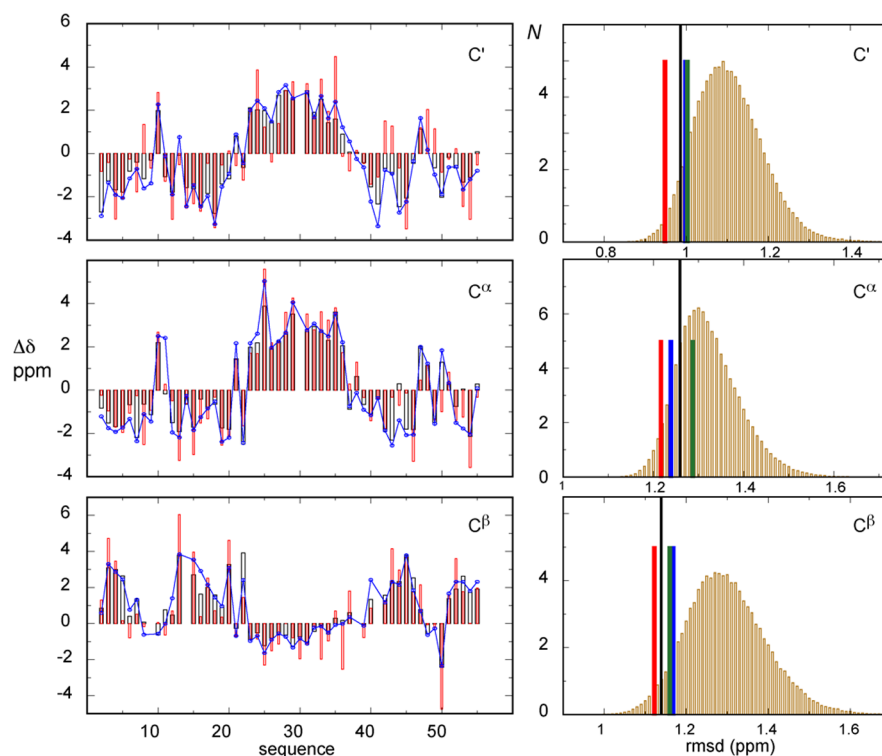


**Figure 2.** Reproduction of CSs from a 200 ns trajectory of microcrystalline GB1. Left: Experimental secondary shifts (red), compared to the ensemble average (blue) and 2GI9 (black). Right: Distribution of rmsds of calculated and experimental CSs. Orange, individual snapshots; black, 2GI9; red, average over all snapshots; green, average over the single structure; blue, average over the same structure with neighboring molecules included.

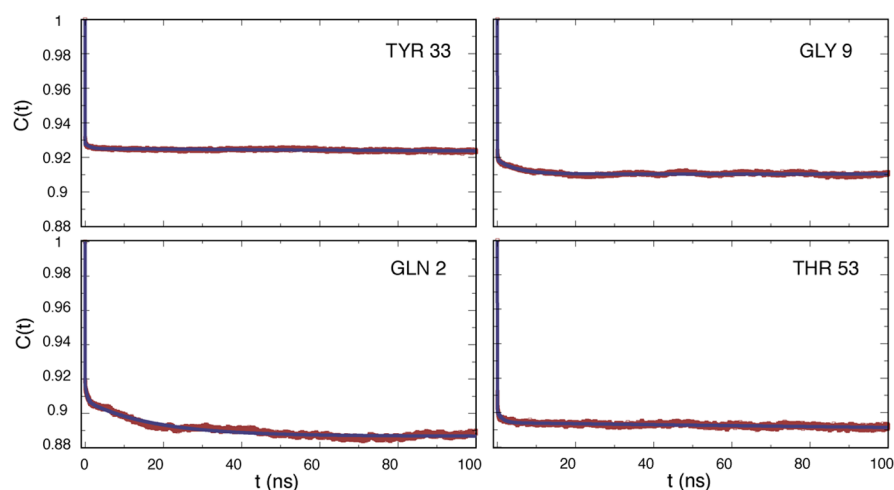


**Figure 3.** Examples of angular correlation functions (red) for NH bond vectors for four amino acids in four different copies of GB1 (the fit to eq 1 with  $n = 3$  is shown in blue).

where  $\sum A = 1$  and  $\tau_k$  are the exponential time constants. Spectral density functions are then calculated as

$$J(\omega) = \sum_{k=1}^n \frac{A_k 2\tau_k}{1 + (\omega\tau_k)^2} \quad (2)$$

Note that  $n = 2$  for the so-called extended model-free (EMF) approach,<sup>33</sup> while  $n = 1$  for the simple model-free (SMF) approach (Supporting Information).  $A_0$  expresses the overall degree of motion, defining the plateau value of the correlation function, and is equivalent to  $S^2$  in the MF approaches (similarly  $1 - A_1$  is equivalent to the EMF  $S_f^2$ ).<sup>34</sup> Examples of correlation functions and fits using eq 1 with  $n = 3$  are shown in Figure 3 (see the Supporting Information for a table of fitted values). Most residues exhibit a larger amplitude motion with  $\tau < 10$  ps, with additional components on both the 1 and 20 ns time scales. Resulting MD-derived relaxation rates are compared to experimental  $^{15}\text{N}$   $R_1$  and  $R_{1\rho}$  measured at 23.5 T ( $\omega_{\text{H}}/2\pi = 1$  GHz) (Figure 4).<sup>19</sup> The distribution of simulated  $R_1$  rates is in broad agreement with experiment, although underestimated.  $R_{1\rho}$  is more severely underestimated, possibly due to the relatively short simulation (200 ns) compared to the time scale of events that could contribute to this rate.<sup>35</sup> Indeed, despite the overall stability of the simulation, a relatively high proportion (10%) of residues exhibit statistically rare dynamic events, giving rise to poorly converged correlation functions that cannot be fitted by eq 1, and are therefore not included in the calculated rates, providing evidence from both experiment and simulation that backbone dihedral flips still occur in crystalline proteins on time scales slower than those sampled here (Supporting Information).

Fitting dynamic parameters to experimental relaxation rates is generally poorly determined due to the low number of rates that can be measured, so that experimental data are often fitted using the SMF or EMF approaches. Figure 4C shows  $S^2$  values determined from experiment using SMF, compared to  $A_0$  extracted from simulation. Despite notable discrepancies in the region of 10–14, the profiles determined from MD and relaxation times are similar, including the highly dynamic Gly 41 and higher  $S^2$  in  $\beta$ -strands 1, 3, and 4 and the  $\alpha$ -helix as compared to that for  $\beta 2$ . However, the level of dynamics, which is similar to that predicted by MD simulation of the

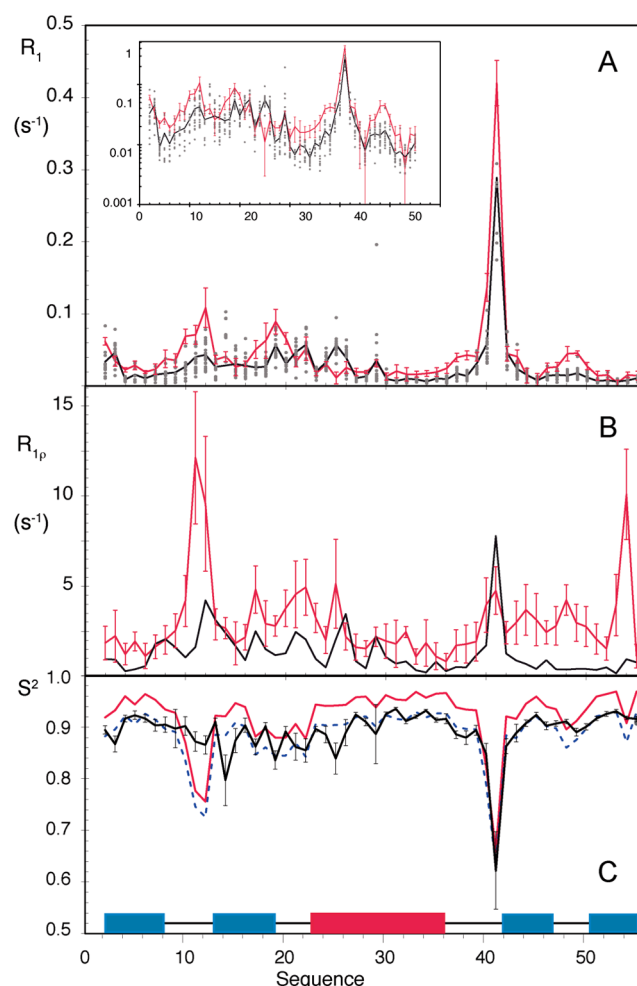


**Figure 4.** (A) Longitudinal (inset, logarithmic plot) and (B) transverse relaxation (black) calculated from 32 trajectories of GB1, compared to experimental data (red) measured at 1 GHz. (C)  $S^2$  derived from experimental  $R_1$  and  $R_{1\rho}$  using SMF (red) and scaled by 0.96 (blue), compared to  $A_0$  derived from fitting all MD trajectories to eq 1 (black). Positions of  $\beta$ -sheets (blue) and  $\alpha$ -helices (red) are shown.

protein in solution (Supporting Information), is higher in the simulation compared to that derived from the SMF analysis of experimental data. Scaling of the  $A_0$  profile derived from simulation indeed identifies that a factor of 0.96 results in a close reproduction of the experimentally derived profile (Figure 4). Using SMF to fit relaxation rates calculated from the simulation (the predicted rates in Figure 4) shows the same underestimation of motional amplitudes (Supporting Information), demonstrating that this effect occurs because SMF cannot sufficiently account for more complex dynamics occurring on more than one time scale. Correlation times of slower motions in the simulation are in reasonable agreement with those determined from SMF analysis, confirming that this model is primarily sensitive to slow components. Although the SMF spectral density function is used here, any model with a single motional mode, such as 1DGAF,<sup>31</sup> or diffusion in a cone,<sup>29</sup> will underestimate the overall amplitude of fast local motion while still fitting experimental relaxation  $R_1$  and  $R_{1\rho}$  values well.

The obvious solution to this problem is to use more complex dynamic models, such as EMF, to interpret the data. Not surprisingly, attempts to fit experimental  $R_1$  and  $R_{1\rho}$  rates using the EMF model result in a highly underdetermined parameter space. In order to remedy this, it has been proposed that the parametric space would be better constrained by measuring dipolar couplings (DCs) to define the appropriate  $S^2$  value for each site.<sup>11,15,16</sup> We have therefore combined DCs from GB1<sup>36</sup> with  $R_1$  (800 MHz, 1 GHz) and  $R_{1\rho}$  (1 GHz) in the fitting procedure for the EMF model. This results in significantly lower  $S_f^2$  values than those found in the MD simulation (Figure 5A), mirroring a recent study of ubiquitin,<sup>16</sup> where larger amplitude fast motions were found than those measured or simulated in solution. Note the dramatic change in the experimental prediction in these different scenarios; without DCs (using SMF), fast order parameters are systematically overestimated (Figure 4C), while using EMF with DCs appears to substantially underestimate the same parameters (Figure 5A).

In order to better understand the origin of this apparent discrepancy, we have mapped the available parametric space associated with fits using EMF (Figure 5B–D). The degeneracy of well-fitting solutions to different combinations of ( $S_f^2$ ,  $S^2$ ,  $\tau_f$  and  $\tau_s$ ) when fitting five relaxation rates is evident (light gray shading). The addition of DCs narrows the range of parameters, in agreement with the data.

Important, however, the precision of the DC is critical for the accuracy of the description. If only 97.5% of the full DC is measured, the analysis still reproduces all synthetic data within reasonable uncertainty but with much lower and therefore incorrect values of  $S_f^2$ . This observation has particular importance when one considers the difficulties of measuring these parameters with 100% accuracy,<sup>37</sup> and it is clear that any systematic underestimation of DCs would lead to overestimation of dynamic amplitudes. The figure also highlights the influence of small-amplitude slower motions (>20 ns) whose correlation times are far from the transition frequencies affecting  $R_1$  but whose presence still strongly influences effective  $S_f^2$  values.

In conclusion, a 200 ns MD simulation of GB1 in its crystalline lattice predicts distributions of longitudinal relaxation rates and chemical shifts in reasonable agreement with experiment, suggesting that both fast and slow conformational properties of the protein are accurately

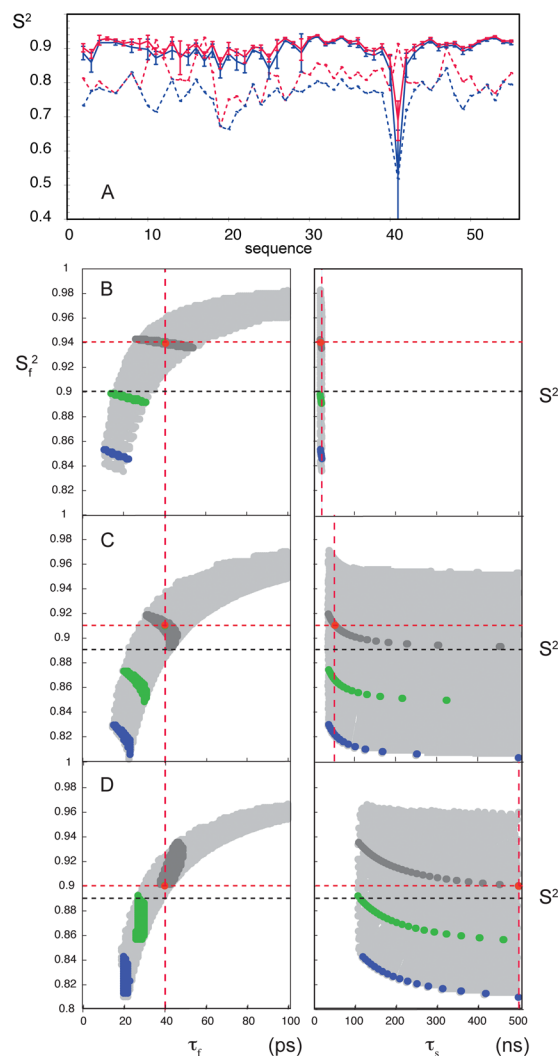


**Figure 5.** (A) Comparison of  $S_f^2$  (red) and  $S^2$  (blue), derived from the MD trajectories (solid lines) and values determined from combined analysis of  $R_1$  (800 MHz, 1 GHz),  $R_{1\rho}$  (1 GHz), and DCs (dashed lines). (B–D) Parametric space available for fits of relaxation data using EMF in the presence and absence of DCs. Light gray: Solutions ( $\chi^2/N < 1$ ) of the fit of  $S_f^2$ ,  $S^2$ ,  $\tau_f$  and  $\tau_s$  to  $R_1$  (500, 600, 800 MHz) and  $R_{1\rho}$  (600, 800 GHz). Dark gray: As above, with DCs used to define  $S^2$ . Green: As above, including DCs scaled by 0.975. Blue: As above, including DCs scaled by 0.95. (B) Target (red dashed lines and point)  $S_f^2 = 0.94$ ,  $S^2 = 0.9$ ,  $\tau_f = 20$  ns. (C)  $S_f^2 = 0.91$ ,  $S^2 = 0.89$ ,  $\tau_s = 50$  ns. (D)  $S_f^2 = 0.9$ ,  $S^2 = 0.89$ ,  $\tau_s = 500$  ns,  $\tau_f = 40$  ps in all targets. All solutions shown reproduce noise-free synthetic data within 5%. Left and right sides show  $S_f^2, \tau_f$  and  $S_f^2, \tau_s$  spaces, respectively.

captured by simulation. Contributions to  $R_{1\rho}$  are less well reproduced, probably due to the relatively short simulation compared to the time scales that can influence  $R_{1\rho}$ . This comparison highlights possible sources of systematic error in the dynamic description incurred when interpreting solid-state relaxation using approaches generally applied in solution. While the extra parameter space available for exploration of slow motions by solid-state NMR is an exciting perspective, more data (or higher accuracy) are required than in analogous solution studies, where the range of relaxation-active time scales is limited by overall tumbling. More generally, this study emphasizes the important role that MD simulation will



play in the interpretation of solid-state NMR studies of protein dynamics.

## ■ ASSOCIATED CONTENT

### Supporting Information

Methods used for MD simulation and analysis. Additional figures. This material is available free of charge via the Internet at <http://pubs.acs.org>.

## ■ AUTHOR INFORMATION

### Corresponding Author

\*E-mail: [martin.blackledge@ibs.fr](mailto:martin.blackledge@ibs.fr).

### Notes

The authors declare no competing financial interest.

## ■ ACKNOWLEDGMENTS

Calculations were performed on the High Performance Computing resources of CCRT. Financial support was from CEA, CNRS, and ANR via ANR-12-BS07-0023-01/Complex-Dynamics (M.B) and the Marie-Curie training program grant number 273786 (L.M.).

## ■ REFERENCES

- (1) Frauenfelder, H.; Sligar, S.; Wolynes, P. The Energy Landscapes and Motions of Proteins. *Science* **1991**, *254*, 1598–1603.
- (2) Lipari, G.; Szabo, A. Model-Free Approach to the Interpretation of NMR Relaxation in Macromolecules. 1. Theory and Range of Validity. *J. Am. Chem. Soc.* **1982**, *104*, 4546–4559.
- (3) Torchia, D. A. Dynamics of Biomolecules from Picoseconds to Seconds at Atomic Resolution. *J. Magn. Reson.* **2011**, *212*, 1–10.
- (4) Mittermaier, A.; Kay, L. E. New Tools Provide New Insights in NMR Studies of Protein Dynamics. *Science* **2006**, *312*, 224–228.
- (5) Salmon, L.; Pierce, L.; Grimm, A.; Roldan, J.-L. O.; Mollica, L.; Jensen, M. R.; Nuland, N.; van; Markwick, P. R. L.; McCammon, J. A.; Blackledge, M. Multi-Timescale Conformational Dynamics of the SH3 Domain of CD2-Associated Protein Using NMR Spectroscopy and Accelerated Molecular Dynamics. *Angew. Chem., Int. Ed.* **2012**, *51*, 6103–6106.
- (6) Szabo, A.; Torchia, D. A. Spin-Lattice Relaxation in Solids. *J. Magn. Reson.* **1982**, *49*, 107.
- (7) Cole, H.; Torchia, D. An NMR-Study of the Backbone Dynamics of Staphylococcal Nuclease in the Crystalline State. *Chem. Phys.* **1991**, *158*, 271–281.
- (8) Giraud, N.; Böckmann, A.; Lesage, A.; Penin, F.; Blackledge, M.; Emsley, L. Site-Specific Backbone Dynamics from a Crystalline Protein by Solid-State NMR Spectroscopy. *J. Am. Chem. Soc.* **2004**, *126*, 11422–11423.
- (9) Giraud, N.; Blackledge, M.; Goldman, M.; Böckmann, A.; Lesage, A.; Penin, F.; Emsley, L. Quantitative Analysis of Backbone Dynamics in a Crystalline Protein from Nitrogen-15 Spin-Lattice Relaxation. *J. Am. Chem. Soc.* **2005**, *127*, 18190–18201.
- (10) Lorieau, J. L.; McDermott, A. E. Conformational Flexibility of a Microcrystalline Globular Protein: Order Parameters by Solid-State NMR Spectroscopy. *J. Am. Chem. Soc.* **2006**, *128*, 11505–11512.
- (11) Chevelkov, V.; Xue, Y.; Linser, R.; Skrynnikov, N. R.; Reif, B. Comparison of Solid-State Dipolar Couplings and Solution Relaxation Data Provides Insight into Protein Backbone Dynamics. *J. Am. Chem. Soc.* **2010**, *132*, 5015.
- (12) Chevelkov, V.; Zhuravleva, A. V.; Xue, Y.; Reif, B.; Skrynnikov, N. R. Combined Analysis of  $^{15}\text{N}$  Relaxation Data from Solid- And Solution-State NMR Spectroscopy. *J. Am. Chem. Soc.* **2007**, *129*, 12594.
- (13) Chevelkov, V.; Diehl, A.; Reif, B. Measurement of  $^{15}\text{N}$ - $T_1$  Relaxation Rates in a Perdeuterated Protein by Magic Angle Spinning Solid-State Nuclear Magnetic Resonance Spectroscopy. *J. Chem. Phys.* **2008**, *128*, 052316.
- (14) Krushelnitsky, A.; Zinkevich, T.; Reichert, D.; Chevelkov, V.; Reif, B. Microsecond Time Scale Mobility in a Solid Protein As Studied by the  $^{15}\text{N}$   $R_{1\rho}$  Site-Specific NMR Relaxation Rates. *J. Am. Chem. Soc.* **2010**, *132*, 11850–11853.
- (15) Chevelkov, V.; Fink, U.; Reif, B. Accurate Determination of Order Parameters from  $^1\text{H}$ ,  $^{15}\text{N}$  Dipolar Couplings in MAS Solid-State NMR Experiments. *J. Am. Chem. Soc.* **2009**, *131*, 14018–14022.
- (16) Schanda, P.; Meier, B. H.; Ernst, M. Quantitative Analysis of Protein Backbone Dynamics in Microcrystalline Ubiquitin by Solid-State NMR Spectroscopy. *J. Am. Chem. Soc.* **2010**, *132*, 15957–15967.
- (17) Lewandowski, J.; Sein, J.; Sass, H.; Grzesiek, S.; Blackledge, M.; Emsley, L. Measurement of Site-Specific  $^{13}\text{C}$  Spin-Lattice Relaxation in a Crystalline Protein. *J. Am. Chem. Soc.* **2010**, *132*, 8252–+.
- (18) Lewandowski, J. R.; Sein, J.; Blackledge, M.; Emsley, L. Anisotropic Collective Motion Contributes to Nuclear Spin Relaxation in Crystalline Proteins. *J. Am. Chem. Soc.* **2010**, *132*, 1246–1248.
- (19) Lewandowski, J. R.; Sass, H. J.; Grzesiek, S.; Blackledge, M.; Emsley, L. Site-Specific Measurement of Slow Motions in Proteins. *J. Am. Chem. Soc.* **2011**, *133*, 16762–16765.
- (20) Knight, M. J.; Pell, A. J.; Bertini, I.; Felli, I. C.; Gonnelli, L.; Pierattelli, R.; Herrmann, T.; Emsley, L.; Pintacuda, G. Structure and Backbone Dynamics of a Microcrystalline Metalloprotein by Solid-State NMR. *Proc. Natl. Acad. Sci. U.S.A.* **2012**, *109*, 11095–11100.
- (21) Levy, R. M.; Karplus, M.; McCammon, J. A. Molecular Dynamics Studies of NMR Relaxation in Proteins. *Biophys. J.* **1980**, *32*, 628–630.
- (22) Brüschweiler, R. New Approaches to the Dynamic Interpretation and Prediction of NMR Relaxation Data from Proteins. *Curr. Opin. Struct. Biol.* **2003**, *13*, 175–183.
- (23) Franks, W. T.; Wylie, B. J.; Stellfox, S. A.; Rienstra, C. M. Backbone Conformational Constraints in a Microcrystalline  $^{15}\text{N}$ -Labeled Protein by 3D Dipolar-Shift Solid-State NMR Spectroscopy. *J. Am. Chem. Soc.* **2006**, *128*, 3154–3155.
- (24) Cerutti, D. S.; Freddolino, P. L.; Duke, R. E.; Case, D. A. Simulations of a Protein Crystal with a High Resolution X-ray Structure: Evaluation of Force Fields and Water Models. *J. Phys. Chem. B* **2010**, *114*, 12811–12824.
- (25) Li, D.-W.; Brüschweiler, R. Certification of Molecular Dynamics Trajectories with NMR Chemical Shifts. *J. Phys. Chem. Lett.* **2010**, *1*, 246–248.
- (26) Markwick, P. R. L.; Cervantes, C. F.; Abel, B. L.; Komives, E. A.; Blackledge, M.; McCammon, J. A. Enhanced Conformational Space Sampling Improves the Prediction of Chemical Shifts in Proteins. *J. Am. Chem. Soc.* **2010**, *132*, 1220–1221.
- (27) Berjanskii, M. V.; Wishart, D. S. A Simple Method to Predict Protein Flexibility Using Secondary Chemical Shifts. *J. Am. Chem. Soc.* **2005**, *127*, 14970–14971.
- (28) Robustelli, P.; Stafford, K. A.; Palmer, A. G. Interpreting Protein Structural Dynamics from NMR Chemical Shifts. *J. Am. Chem. Soc.* **2012**, *134*, 6365–6374.
- (29) Neal, S.; Nip, A. M.; Zhang, H.; Wishart, D. S. Rapid and Accurate Calculation of Protein  $^1\text{H}$ ,  $^{13}\text{C}$  and  $^{15}\text{N}$  Chemical Shifts. *J. Biomol. NMR* **2003**, *26*, 215–240.
- (30) Shen, Y.; Bax, A. SPARTA+: A Modest Improvement in Empirical NMR Chemical Shift Prediction by Means of an Artificial Neural Network. *J. Biomol. NMR* **2010**, *48*, 13–22.
- (31) Bremi, T.; Brüschweiler, R. Locally Anisotropic Internal Polypeptide Backbone Dynamics by NMR rRelaxation. *J. Am. Chem. Soc.* **1997**, *119*, 6672–6673.
- (32) Showalter, S. A.; Brüschweiler, R. Validation of Molecular Dynamics Simulations of Biomolecules Using NMR Spin Relaxation As Benchmarks: Application to the AMBER99SB Force Field. *J. Chem. Theory Comput.* **2007**, *3*, 961–975.
- (33) Clore, G.; Szabo, A.; Bax, A.; Kay, L.; Driscoll, P.; Gronenborn, A. Deviations from the Simple 2-Parameter Model-

Free Approach to the Interpretation of  $^{15}\text{N}$  Nuclear Magnetic-Relaxation of Proteins. *J. Am. Chem. Soc.* **1990**, *112*, 4989–4991.

(34) Chandrasekhar, I.; Clore, G.; Szabo, A.; Gronenborn, A.; Brooks, B. A 500-ps Molecular-Dynamics Simulation Study of Interleukin-1-Beta in Water — Correlation with Nuclear-Magnetic-Resonance Spectroscopy and Crystallography. *J. Mol. Biol.* **1992**, *226*, 239–250.

(35) Tollinger, M.; Sivertsen, A. C.; Meier, B. H.; Ernst, M.; Schanda, P. Site-Resolved Measurement of Microsecond-to-Millisecond Conformational-Exchange Processes in Proteins by Solid-State NMR Spectroscopy. *J. Am. Chem. Soc.* **2012**, *134*, 14800–14807.

(36) Wylie, B. J.; Sperling, L. J.; Nieuwkoop, A. J.; Franks, W. T.; Oldfield, E.; Rienstra, C. M. Ultrahigh Resolution Protein Structures Using NMR Chemical Shift Tensors. *Proc. Natl. Acad. Sci. U.S.A.* **2011**, *108*, 16974–16979.

(37) Schanda, P.; Meier, B. H.; Ernst, M. Accurate Measurement of One-Bond H–X Heteronuclear Dipolar Couplings in MAS Solid-State NMR. *J. Magn. Reson.* **2011**, *210*, 246–259.

#### ■ NOTE ADDED AFTER ASAP PUBLICATION

This paper was published ASAP on November 27, 2012. Equation 1 was updated. The revised paper was reposted on November 28, 2012.